JACS
JOURNAL OF THE AMERICAN CHEMICAL SOCIETY
Article
pubs.acs.org/JACS

Wirelike Charge Transport Dynamics for DNA–Lipid Complexes in Chloroform

Ashutosh Kumar Mishra, Ryan M. Young, Michael R. Wasielewski,* and Frederick D. Lewis*

Department of Chemistry and Argonne-Northwestern Solar Energy Research (ANSER) Center, Northwestern University, Evanston, Illinois 60208-3113, United States

Supporting Information

ABSTRACT: The dynamics of charge separation and charge recombination have been determined for lipid complexes of DNA capped hairpins possessing stilbene electron-acceptor and -donor chromophores separated by base-pair domains that vary in length and base sequence in chloroform solution by means of femtosecond time-resolved transient absorption spectroscopy. The results obtained for the DNA–lipid complexes are compared with those previously obtained in our laboratories for the same hairpins in aqueous buffer. The charge separation and charge recombination times for the lipid complexes are consistently much shorter than those determined in aqueous solution and are only weakly dependent on the number of base pairs separating the acceptor and donor. The enhanced rate constants for forward and return charge transport in DNA–lipid complexes support proposals that solvent gating is responsible, to a significant extent, for the relatively low rates of charge transport for DNA in water. Moreover, they suggest that DNA–lipid complexes may prove useful in the development of DNA-based molecular electronic devices.

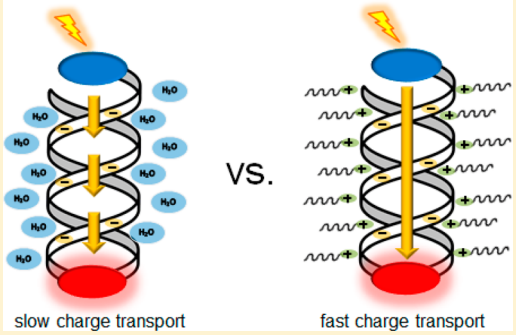

INTRODUCTION

Compared with electron transfer in conductive organic materials,[1] charge transport in DNA in aqueous solution is an intrinsically slow process.[2,3] The highest hole transport rates have been observed for polypurine sequences.[4] We have employed femtosecond time-resolved transient absorption spectroscopy to determine the rate constants for charge transport from a donor stilbene (Sd) to an excited acceptor stilbene (^{1}Sa*) separated by a variable number of A-T base pairs (Chart 1a,d).[5,6] Kinetic modeling of the hole transit times for longer A-tracts provided a rate constant of 1.2×10^9 s^{-1} for A-to-A hole hopping.[7] A somewhat higher rate constant for G-to-G hole transport, 4.2×10^9 s^{-1}, was obtained from the hole transit times for Sa–Sd-capped hairpin systems in which the A-tract was replaced by an A_mG_n diblock purine (m = 2 or 3, n = 2–19; Chart 1e).[8,9] Even higher rate constants for hole transport have been reported for some nucleobase analogues.[2,3] Kawai and Majima[3] reported rate constants of 0.4×10^8 and 3.8×10^8 s^{-1} for hole transport between guanines in alternating $(GA)_n$ and $(GC)_n$ sequences, respectively. Even lower rate constants were observed for nonalternating base sequences.[3]

Our experimental values of the A-to-A and G-to-G hole hopping rate constants (k_{hop}) are similar to those calculated by Steinbrecher et al.[10] using a QM/MM model that explicitly considered solvent interactions. To place these values in context, they are similar to the experimental value for poly(*N*-vinylcarbazole) in dichloromethane (1.1×10^9 s^{-1}) and larger than the value for polystyrene ($\leq 10^7$ s^{-1}).[11] A hole mobility (μ) of 5×10^{-3} cm^2 V^{-1} s^{-1} has been reported for charge recombination in the lipid complex of a 13-mer DNA duplex having a $A_5G_3A_5$ poly(purine) strand based on time-resolved microwave conductivity measurements in CCl_4.[12] This value is substantially larger than the value $\mu = 2 \times 10^{-5}$ cm^2 V^{-1} s^{-1} estimated by Senthilkumar et al.[13] for hole mobility in a poly(A) stack in aqueous solution.

Theoretical analyses of charge transport in DNA have provided several possible explanations for its relatively low hole mobility in aqueous solution. These include "gating" processes such as base-pair motion,[14,15] counterion motion,[16] and solvent fluctuations.[17] Incorporation of locked nucleic acids into duplex structures[18] or binding of Mg^{2+} in the minor groove[19] results in decreased rate constants for hole transport, presumably as a consequence of decreased base-pair conformational mobility.

The effect of solvation on the dynamics of electron transfer in proteins has been extensively investigated.[20] Incorporation of redox-active proteins into lipid bilayers can have a pronounced influence on electron transfer reaction rates as a consequence of control over the mode of interaction between proteins.[21] Virtually all studies of DNA charge transport dynamics have been conducted in aqueous solution, with the exception of the lipid complex study mentioned above.

We report here the results of an investigation of photoinduced charge transport in the complexes of hexadecyltrimethylammonium bromide (CTAB) with the Sa/Sd systems shown in Chart 1 in chloroform solution. The dynamics of

Received: September 13, 2014
Published: October 9, 2014

   dx.doi.org/10.1021/ja509456q | J. Am. Chem. Soc. 2014, 136, 15792–15797

Chart 1. Structures of (a) the Sa Stilbenedicarboxamide Capping Group and Sd Stilbenediether Hairpin Linker, (B) the Purines Adenine and Guanine, (c) CTAB, and (d–f) Capped Hairpins Having (d) Poly(A), (e) Diblock A_2G_n, and (f) Varied Base Sequences

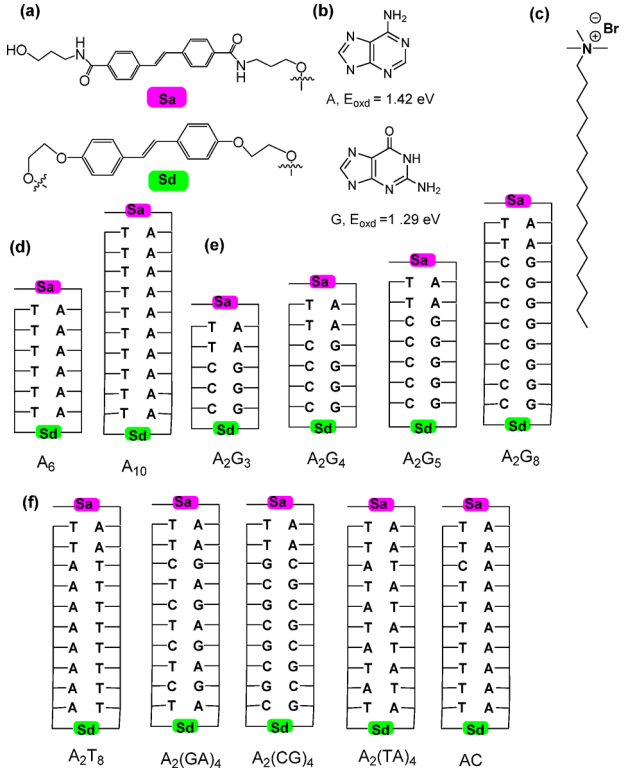

charge separation and charge recombination are significantly faster for the lipid complexes than for the noncomplexed systems in aqueous buffer. Higher rate constants, ease of preparation, and protection from strand cleavage reactions[22] make DNA–lipid complexes promising materials for applications in molecular electronic devices and potential models for electron transport in DNA–enzyme complexes.[22,23]

RESULTS AND DISCUSSION

Synthesis and Steady-State Spectra. The capped hairpins whose structures are shown in Chart 1 were prepared, purified, and characterized as described previously (see Materials and Methods).[5,8] The hairpins were converted to their CTAB complexes following the procedure of Ijiro and Okahata,[24] dried in vacuum, and dissolved in chloroform. The UV and circular dichroism (CD) spectra of several CTAB complexes are shown in Figure 1. The other CTAB complexes have similar spectra (data not shown). Absorption by the solvent restricts these spectra to wavelengths longer than 245 nm. The UV spectra of the CTAB complexes display long-wavelength bands assigned to overlapping absorption of the Sa and Sd chromophores and short-wavelength bands assigned to overlapping absorption of the DNA bases and stilbenes. The ratio of the short- and long-wavelength band intensities increases as the number of base pairs in the hairpin increases. The UV spectra of the A_2G_n–CTAB solutions remain essentially unchanged over the temperature range 5–60 °C (Figures S1 and S2 in the Supporting Information). The capped hairpins all have melting transitions above 60 °C in aqueous solution.[8]

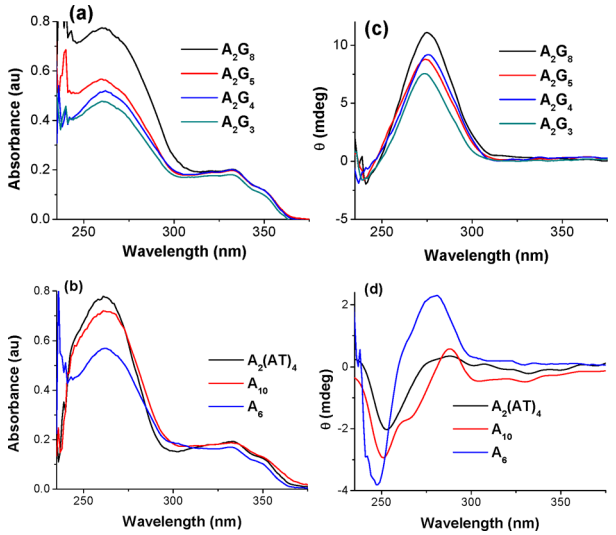

Figure 1. (a, b) UV–vis absorption spectra and (c, d) circular dichroism spectra of CTAB complexes in $CHCl_3$ solution. The solvent absorbs strongly at wavelengths shorter than 250 nm.

The CD spectra of A_2G_n–CTAB complexes shown in Figure 1c display a positive band at 275 ± 1 nm and a negative band near the solvent cutoff. CD spectra similar to those for the A_2G_n complexes have been reported for several DNA–lipid complexes, including the duplex studied by Yamagami et al.[12,25] The CD spectra of the CTAB complexes of A_6, A_{10}, and $A_2(TA)_4$ shown in Figure 1d also display long-wavelength maxima and short-wavelength minima; however their band intensities are dependent upon the base sequence. There is general agreement that duplex DNA retains a helical geometry in its lipid complexes; however, whether short synthetic duplexes adopt a classical B-DNA structure or some variant is uncertain.

The fluorescence spectra of the hairpin–CTAB solutions in $CHCl_3$ and A_2G_n in aqueous buffer are shown in Figure S3. We assign the fluorescence to the Sa chromophore on the basis of highly efficient quenching of the Sd fluorescence by G-C base pairs in Sd-linked hairpins.[26] The spectra of the CTAB complexes have band maxima at 382 ± 1 nm, which are slightly higher in energy than the maxima of the hairpins in aqueous solution (386 nm).[27] The spectra of the CTAB complexes also display vibronic structure similar to that of the isolated Sa linker, whereas the spectra of the hairpins in buffer are structureless.[27] The structured Sa fluorescence suggests that the electronic interaction of Sa with the adjacent A-T base pair is weaker in the CTAB complex than in aqueous solution, plausibly as a consequence of the absence of hydrophobic attraction.

The fluorescence quantum yields (Φ_f) for the CTAB complexes in $CHCl_3$ are reported in Table 1 along with available values for the capped hairpins in aqueous buffer.[5] The relatively large quantum yields for the A_n capped hairpins in buffer are attributed to delayed fluorescence from reversibly formed $Sa^{-\bullet}A^{+\bullet}$ contact radical ion pairs or exciplexes.[5] The much lower values for A_2G_n hairpins in buffer, like the low values for Sa-linked hairpins with a neighboring AAG sequence, are attributed to trapping of the $A^{+\bullet}$ radical cation by G.[27] Values of $0.13 \geq \Phi_f \geq 0.05$ were obtained for all of the CTAB complexes. The similar values of Φ_f are consistent with the absence of delayed fluorescence for the CTAB complexes.

dx.doi.org/10.1021/ja509456q | J. Am. Chem. Soc. 2014, 136, 15792–15797

Table 1. Quantum Yields for Fluorescence and Charge Separation and Kinetics for Charge Separation and Charge Recombination for CTAB Complexes of Sa/Sd-Capped Hairpins in $CHCl_3$ from This Study and Literature Values for the Capped Hairpins in Aqueous Buffer[a]

hairpin	medium	Φ_f	Φ_{cs}	τ_{cs} (ps)	τ_{cr} (ns)
A_6	CTAB	0.10	0.29	206 ± 16	7.01 ± 0.80
	buffer	0.31[b]	0.09[c]	9000[c]	1.4 × 10^5[c]
A_{10}[d]	CTAB	0.08	0.32	150 ± 20	
A_2G_3	CTAB	0.05	0.29	165 ± 13	6.79 ± 0.75
	buffer	0.009	0.34[c]	490[c]	
A_2G_4	CTAB	0.07	0.31	174 ± 15	5.16 ± 0.52
	buffer	0.010	0.32[c]	1000[c]	
A_2G_5	CTAB	0.09	0.28	214 ± 19	6.40 ± 0.78
	buffer	0.012	0.25[c]	1700[c]	
A_2G_8	CTAB	0.10	0.29	231 ± 20	5.94 ± 0.70
	buffer	0.013	0.24[c]	5000[c]	
A_2T_8	CTAB	0.13	0.35	366 ± 27	7.64 ± 0.97
$A_2(GA)_4$	CTAB	0.11	0.33	234 ± 22	4.80 ± 0.57
$A_2(CG)_4$	CTAB	0.11	0.32	362 ± 37	3.67 ± 0.42
$A_2(TA)_4$	CTAB		<0.02		
AC	CTAB	0.13	0.32	326 ± 30	6.77 ± 0.96

[a]Aqueous buffer: 0.1 M NaCl and 10 mM sodium phosphate, pH 7.2. Data are from this study except as noted. Charge separation was not observed for A_{10} in aqueous buffer or for CTAB–$A_2(TA)_4$. [b]Data from ref 7. [c]Data from ref 10. [d]A satisfactory fit was not obtained for τ_{cr}.

Transient Absorption Spectra. Femtosecond time-resolved transient absorption spectra were obtained as previously described using 350 nm excitation (for selective excitation of Sa vs Sd) from a Ti-sapphire-based system having a time resolution of ca. 180 fs, a spectral range of 440–800 nm, and a time window of 0–7 ns.[28] Typical transient absorption spectra for the CTAB complexes in Chart 1 are shown in Figure 2 for A_2G_8–CTAB, and the transient spectra of the other CTAB complexes are provided in Figures S4–S13 in the Supporting Information. The single band observed with a maximum at 591 ± 1 nm at short delay times is assigned to the ^{1}Sa* singlet state. The decay of this band is accompanied by band broadening, a shift of the band maximum to shorter wavelength (attributed to reduction of ^{1}Sa* to $Sa^{-\bullet}$), and the formation of a second band at 538 ± 1 nm (assigned to $Sd^{+\bullet}$, which does not display a time-dependent change in band shape). Only in the case of $A_2(TA)_4$–CTAB is the band assigned to $Sd^{+\bullet}$ not detected. The broadening and blue shift observed for the $Sa^{-\bullet}$ bands of the CTAB complexes are not observed in aqueous buffer.[8] The formation of the band assigned to $Sd^{+\bullet}$ is observed for A_6 and the A_2G_n diblock hairpins in aqueous solution, but not for A_{10} or for alternating sequences such as $A_2(TA)_4$ and $A_2(GA)_4$.[8,29] Hairpins possessing 10 base pairs with a single crossover (A_2T_8) or mismatch (AC) have not been studied in buffer but are not expected to undergo charge separation in buffer on the time scale of our measurements.

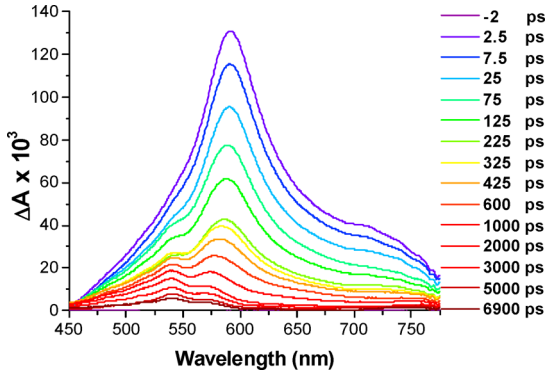

Figure 2. Transient spectra of A_2G_8–CTAB in $CHCl_3$ at delay times from −0.2 ps to 6.9 ns.

The transient spectra of the CTAB complexes in $CHCl_3$ between 440 and 800 nm at 0–7 ns were subjected to singular value decomposition (SVD) and global fitting to the kinetic model A → B → ground state, which is a simplified version of the mechanism previously proposed for charge separation in A_6 shown in Scheme 1a.[29,30] The spectra associated with the kinetic components A and B for A_2G_8–CTAB, where A is the singlet state ^{1}Sa* and B is the charge-separated state $Sa^{-\bullet}/Sd^{+\bullet}$, are shown in Figure 3a. The species-associated spectra and kinetic fits for the other hairpin–CTAB complexes are shown in Figure S14 in the Supporting Information. While the fits recover the generalized behavior of charge separation in these systems, the agreement of the fits to the principal components is not perfect. This is a result of the oversimplification of the A → B → ground state model, which glosses over the intermediate hole-hopping steps as well as exciplex formation, charge recombination, and fluorescence (Scheme 1a). Nonetheless, the reconstructed spectra (Figures 3a and S14) are in good agreement with the established spectra of Sa*, $Sa^{-\bullet}$, and $Sd^{+\bullet}$.[5] Despite the discrepancies in the fits at intermediate stages (Figures 3b and S14), by deconvoluting the evolution of the spectral components we can more accurately determine the charge separation times for these systems than by the method used previously, which fits the ratio of $Sd^{+\bullet}$ and $Sa^{-\bullet}$ band intensities to a first-order rise,[5,8] which is complicated here by the time-dependent blue shift in the Sa* band. The fits to the kinetic model are shown in Figures 3b and S14, and the decay times for charge separation (A → B, τ_{cs}) and charge

Scheme 1. Mechanisms of Charge Separation and Charge Recombination for (a) the Capped Hairpin A_6 in Aqueous Buffer[29,30] and (b) the CTAB Complex of A_6 in Chloroform

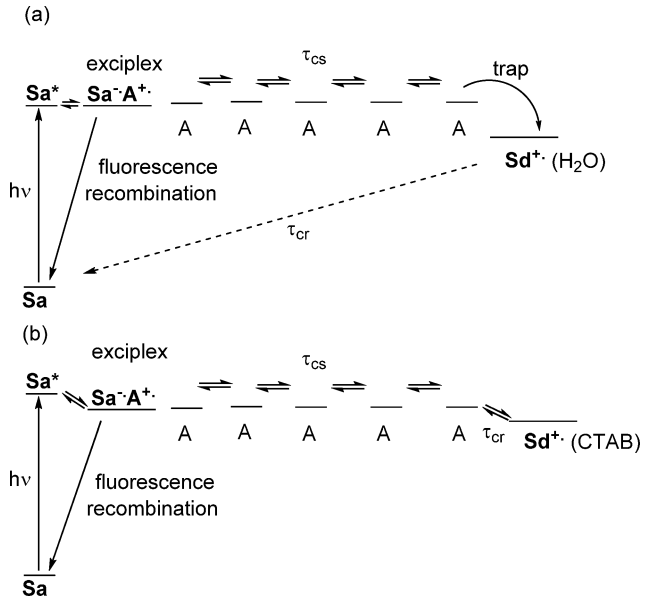

dx.doi.org/10.1021/ja509456q | J. Am. Chem. Soc. 2014, 136, 15792–15797

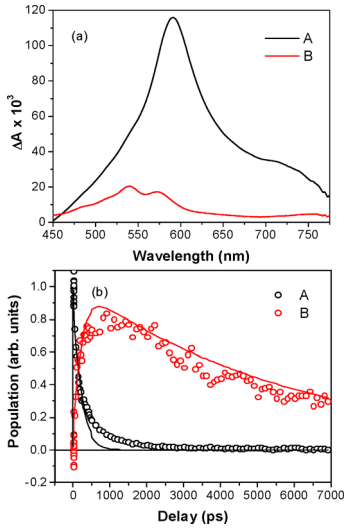

Figure 3. (a) Species-associated spectra for the initial and charge-separated states of A_2G_8 and (b) SVD/global fit to the simplified kinetic model A → B → ground state. A is ^{1}Sa* and B is $Sa^{-\bullet}Sd^{+\bullet}$.

recombination (B → ground state, τ_{cr}) for the CTAB complexes are reported in Table 1. Also reported are values of τ_{cs} and τ_{cr} for some of the hairpins in aqueous buffer.[5,8] For complexes having 10 base pairs, the values of τ_{cs} decrease in the order $A_{10} < A_2(AG)_4 < AC \approx A_2T_8 \approx A_2(CG)_4 < A_2(TA)_4$. The values of τ_{cs} increase slightly with duplex length for the CTAB complexes of the A_2G_n hairpins but decrease for A_{10} versus A_6. The values of τ_{cr} also show relatively small variation with length or base sequence. In view of the fitting errors of our SVD analysis, we do not consider the small differences in τ_{cs} or τ_{cr} to be significant. Much larger differences in the values of τ_{cs} were observed for the A_2G_n hairpins in buffer. Values of τ_{cr} have not been determined for the A_2G_n hairpins in buffer; however, their charge-separated states do not undergo appreciable charge recombination during the 0−7 ns time window of our measurements.[8] Quantum yields for charge separation (Φ_{cs}) for the lipid complexes were determined by comparing the integrated areas of ^{1}Sa* at t = 0 fs and $Sa^{-\bullet}/Sd^{+\bullet}$ at its maximum value (1.5−2 ns). The values of Φ_{cs} reported in Table 1 are similar for all of the lipid complexes (0.32 ± 0.03), with the exception of $A_2(TA)_4$, which fails to undergo detectable charge separation.

The pronounced effect of lipid complexation on the dynamics of charge separation for the Sa/Sd hairpins can be discussed using the modified mechanism shown in Scheme 1b for the A_6 hairpin. For the A_6 hairpin in buffer, it was possible to resolve the fast initial exciplex formation and slower charge separation steps (≤ 30 ps and 9 ns, respectively; Scheme 1a),[30] whereas for the lipid complex only the charge separation step is resolved (cf. Figure 3b). This difference plausibly reflects much faster hole transport and/or hole trapping by Sd for the lipid complex. Much faster hole transport can also account for the very weak distance dependence of τ_{cs} for the A_2G_n hairpins and the similar values of τ_{cs} for the diblock sequence A_2G_8 and the alternating poly(purine) sequence $A_2(GA)_4$, even though the shorter $A_2(GAGAG)$ sequence hairpin fails to undergo measurable charge separation in buffer. Somewhat slower charge separation is observed for the CTAB complexes of sequences that possess a mismatch or strand crossing (AC and A_2T_8) in a poly(purine) sequence or a $(GC)_4$ alternating sequence, (Table 1). Only the CTAB complex possessing an $(AT)_4$ alternating sequence fails to undergo detectable hole transport. Hairpins with this sequence have previously been observed to undergo much less efficient hole transport than poly(A) sequences. A hairpin with the shorter ATATA base sequence undergoes slow, inefficient charge separation in buffer.[29]

The decrease in the charge recombination time for A_6 in lipid versus buffer (τ = 7.3 ns vs 140 μs) is even more pronounced than the decrease in its charge separation time. Charge recombination times for Sa−A_n−Sd and other DNA charge-separated systems in aqueous buffer are moderately distance-dependent ($\beta \approx 0.4$ Å^{-1}) over distances of four to eight A-T base pairs.[5,31] It should be noted that the relative yields of DNA strand cleavage may become independent of distance beyond four base pairs,[4] even though the rate constants for charge separation and charge recombination remain distance-dependent in aqueous buffer.[8]

The absence of a pronounced distance dependence for charge recombination as well as charge separation in hairpin−CTAB complexes suggests that the rate-determining step is neither single-step superexchange nor incoherent hopping, both of which would be expected to display distance dependence.[32] Plausibly, the rate-determining steps for forward and return charge transport are hole trapping by Sd and thermal detrapping, respectively (Scheme 1b). Similar rate-determining steps for all of the hairpins could account for their similar quantum yields for fluorescence and charge separation as well as their similar values of τ_{cs} and τ_{cr} (Table 1). A difference in free energy of ca. 2.0 kcal/mol between the oxidized bridge and $Sd^{+\bullet}$ could account for the higher rate constants for charge separation versus charge recombination.

CONCLUSIONS

In summary, we have observed fast photoinduced charge separation and charge recombination in lipid complexes of capped DNA hairpins in chloroform solution. The hairpins studied differ in length (5−10 base pairs) and base sequence, including duplexes that possess poly(purine) and alternating purine−pyrimidine sequences and sequences having a purine strand crossover and a base-pair mismatch. The observation of fast charge recombination is consistent with the report of high charge mobility for a 13-mer poly(purine)−poly(pyrimidine) duplex with dimethyldipalmitylammonium bromide by Yamagami et al.[12] based on microwave conductivity measurements of charge recombination.

Our results indicate that hole transport in the CTAB complexes is much faster than in aqueous solution and is not the rate-determining step for photoinduced charge separation in the CTAB complexes. It is interesting to note that Renaud et al.[33] have proposed a mechanism for charge separation in the A_6 hairpin in aqueous solution in which the rate-determining step is hole trapping by Sd. If hole trapping is in fact the rate-determining step for charge separation, then hole transport across 5−10 base pairs in the CTAB complexes must be even faster than the charge separation times that we have determined experimentally. Whereas the origin of the rate enhancement for hole transport in lipid complexes versus aqueous solution remains to be elucidated, changes in duplex structure and solvation appear to be contributing factors. Both the CD and fluorescence spectra of the lipid complexes are consistent with less-rigid structures for the lipid complexes, and removal of water from the duplex major and minor grooves should favor

dx.doi.org/10.1021/ja509456q | J. Am. Chem. Soc. 2014, 136, 15792−15797

charge delocalization and lower the activation energy for hole migration.[14,34]

The observation of fast, reversible hole transport in DNA in nonaqueous environments substantially expands the potential utility of DNA in molecular electronic devices and may also account for reports of fast DNA electron transport in protein−DNA complexes.[23,35]

MATERIALS AND METHODS

Materials. The capped hairpins listed in Chart 1 were prepared, purified, and characterized as previously described.[8,36] Values of m/z obtained from MALDI-TOF mass spectrometry are reported in Table S1 in the Supporting Information. The hairpins were converted to their complexes with CTAB following a reported procedure,[24] dried in vacuum, and dissolved in chloroform. All of the subsequent studies were performed in chloroform.

Methods. Fluorescence spectra were recorded for samples (optical density of 0.09 at 350 nm in 1 mL of $CHCl_3$) excited at 350 nm, and the emission spectra were recorded in the range from 365 to 680 nm. Fluorescence quantum yields (Φ_f) were determined relative to the quantum yield of quinine sulfate.[37] CD spectra were recorded on Jasco J-815 CD spectrometer.

Transient absorption spectra were recorded using a previously described apparatus.[28] Samples were stirred during irradiation to minimize the effects of local heating and sample degradation. Transient absorption experiments were performed two or three times on each hairpin, and the results of the individual experiments were similar. However, because of instabilities in the laser system, the signal-to-noise ratio for some of the data prevented them from being fit accurately using the SVD global analysis described below, a problem which was not evident until the analysis was performed. Therefore, the reported time constants and standard errors reported in Table 1 were obtained directly from the SVD analysis of the single set of transient absorption spectra shown in the Supporting Information.

SVD analysis of transient absorption spectra was performed in MATLAB using a laboratory-written program. The 2D spectra were deconvoluted by SVD to produce an orthonormal set of basis spectra that describe the wavelength dependence of the species and a corresponding set of orthogonal vectors that describe the time-dependent amplitudes of the basis spectra.[38] A species-associated first-order kinetic model[39] was fit to a linear combination of the time-dependent amplitude vectors, and the same linear combination of basis spectra was used to construct the spectra for the chemical species.

ASSOCIATED CONTENT

Supporting Information

Mass spectral data, temperature-dependent UV spectra, and transient absorption spectra. This material is available free of charge via the Internet at http://pubs.acs.org.

AUTHOR INFORMATION

Corresponding Authors

m-wasielewski@northwestern.edu
fdl@northwestern.edu

Notes

The authors declare no competing financial interest.

ACKNOWLEDGMENTS

This research was funded by the Office of Naval Research (MURI Grant N00014-11-1-0729). The authors thank Dr. Michelle A. Harris for assistance with the femtosecond transient measurements.

REFERENCES

(1) (a) van de Craats, A. M.; Warman, J. M.; de Haas, M. P.; Adam, D.; Simmerer, J.; Haarer, D.; Schuhmacher, P. *Adv. Mater.* **1996**, *8*, 823. (b) van de Craats, A. M.; Warman, J. M. *Adv. Mater.* **2001**, *13*, 130.
(2) Lewis, F. D. *Isr. J. Chem.* **2013**, *53*, 350.
(3) Kawai, K.; Majima, T. *Acc. Chem. Res.* **2013**, *46*, 2616.
(4) (a) Giese, B.; Amaudrut, J.; Köhler, A.-K.; Spormann, M.; Wessely, S. *Nature* **2001**, *412*, 318. (b) Liu, C.-S.; Hernandez, R.; Schuster, G. B. *J. Am. Chem. Soc.* **2004**, *126*, 2877.
(5) Lewis, F. D.; Zhu, H.; Daublain, P.; Fiebig, T.; Raytchev, M.; Wang, Q.; Shafirovich, V. *J. Am. Chem. Soc.* **2006**, *128*, 791.
(6) Lewis, F. D.; Zhu, H.; Daublain, P.; Cohen, B.; Wasielewski, M. R. *Angew. Chem., Int. Ed.* **2006**, *45*, 7982.
(7) Blaustein, G. S.; Lewis, F. D.; Burin, A. L. *J. Phys. Chem. B* **2010**, *114*, 6732.
(8) Vura-Weis, J.; Wasielewski, M. R.; Thazhathveetil, A. K.; Lewis, F. D. *J. Am. Chem. Soc.* **2009**, *131*, 9722.
(9) Mickley Conron, S. M.; Thazhathveetil, A. K.; Wasielewski, M. R.; Burin, A. L.; Lewis, F. D. *J. Am. Chem. Soc.* **2010**, *132*, 14388.
(10) Steinbrecher, T.; Koslowski, T.; Case, D. A. *J. Phys. Chem. B* **2008**, *112*, 16935.
(11) (a) Miyasaka, H.; Khan, S. R.; Itaya, A. *J. Phys. Chem. A* **2002**, *106*, 2192. (b) Miyasaka, H.; Khan, S. R.; Itaya, A. *J. Photochem. Photobiol., C* **2003**, *4*, 195.
(12) Yamagami, R.; Kobayashi, K.; Saeki, A.; Seki, S.; Tagawa, S. *J. Am. Chem. Soc.* **2006**, *128*, 2212.
(13) Senthilkumar, K.; Grozema, F. C.; Guerra, C. F.; Bickelhaupt, F. M.; Lewis, F. D.; Berlin, Y. A.; Ratner, M. A.; Siebbeles, L. D. A. *J. Am. Chem. Soc.* **2005**, *127*, 14894.
(14) Gutierrez, R.; Caetano, R.; Woiczikowski, P. B.; Kubar, T.; Elstner, M.; Cuniberti, G. *New J. Phys.* **2010**, *12*, No. 023022.
(15) Grozema, F. C.; Tonzani, S.; Berlin, Y. A.; Schatz, G. C.; Siebbeles, L. D. A.; Ratner, M. A. *J. Am. Chem. Soc.* **2008**, *130*, 5157. Voityuk, A. A. *J. Phys. Chem. B* **2009**, *113*, 14365.
(16) Kanvah, S.; Joseph, J.; Schuster, G. B.; Barnett, R. N.; Cleveland, C. L.; Landman, U. *Acc. Chem. Res.* **2010**, *43*, 280.
(17) Kubař, T.; Kleinekathöfer, U.; Elstner, M. *J. Phys. Chem. B* **2009**, *113*, 13107.
(18) (a) Kawai, K.; Hayashi, M.; Majima, T. *J. Am. Chem. Soc.* **2012**, *134*, 9406. (b) Thazhathveetil, A. K.; Vura-Weis, J.; Trifonov, A. A.; Wasielewski, M. R.; Lewis, F. D. *J. Am. Chem. Soc.* **2012**, *134*, 16434.
(19) Thazhathveetil, A. K.; Trifonov, A. A.; Wasielewski, M. R.; Lewis, F. D. *J. Phys. Chem. A.* **2014**, DOI: 10.1021/jp502974s.
(20) Gray, H. B.; Winkler, J. R. In *Electron Transfer in Chemistry*; Balzani, V., Ed.; Wiley-VCH: Weinheim, Germany, 2001; Vol. *3*, p 3.
(21) Cheddar, G.; Tollin, G. *Arch. Biochem. Biophys.* **1994**, *310*, 392.
(22) Cao, H.; Schuster, G. B. *Bioconjugate Chem.* **2005**, *16*, 820.
(23) Sontz, P. A.; Muren, N. B.; Barton, J. K. *Acc. Chem. Res.* **2012**, *45*, 1792.
(24) Ijiro, K.; Okahata, Y. *J. Chem. Soc., Chem. Commun.* **1992**, 1339.
(25) (a) Zhang, T.; Qu, J.; Ogata, N.; Masuda, T. *Eur. Polym. J.* **2011**, *47*, 370. (b) Braun, C. S.; Jas, G. S.; Choosakoonkriang, S.; Koe, G. S.; Smith, J. G.; Middaugh, C. R. *Biophys. J.* **2003**, *84*, 1114.
(26) Lewis, F. D.; Liu, X.; Miller, S. E.; Hayes, R. T.; Wasielewski, M. R. *J. Am. Chem. Soc.* **2002**, *124*, 11280.
(27) Lewis, F. D.; Wu, T.; Liu, X.; Letsinger, R. L.; Greenfield, S. R.; Miller, S. E.; Wasielewski, M. R. *J. Am. Chem. Soc.* **2000**, *122*, 2889.
(28) Brown, K. E.; Veldkamp, B. S.; Co, D. T.; Wasielewski, M. R. *J. Phys. Chem. Lett.* **2012**, *3*, 2362.
(29) Lewis, F. D.; Daublain, P.; Cohen, B.; Vura-Weis, J.; Shafirovich, V.; Wasielewski, M. R. *J. Am. Chem. Soc.* **2007**, *129*, 15130.
(30) Lewis, F. D.; Zhu, H.; Daublain, P.; Sigmund, K.; Fiebig, T.; Raytchev, M.; Wang, Q.; Shafirovich, V. *Photochem. Photobiol. Sci.* **2008**, *7*, 534.
(31) (a) Shafirovich, V. Y.; Dourandin, A.; Huang, W.; Luneva, N. P.; Geacintov, N. E. *Phys. Chem. Chem. Phys.* **2000**, *2*, 4399. (b) Takada, T.; Kawai, K.; Fujitsuka, M.; Majima, T. *Proc. Natl. Acad. Sci. U.S.A.* **2004**, *101*, 14002.
(32) Jortner, J.; Bixon, M.; Langenbacher, T.; Michel-Beyerle, M. E. *Proc. Natl. Acad. Sci. U.S.A.* **1998**, *95*, 12759.

(33) Renaud, N.; Berlin, Y. A.; Lewis, F. D.; Ratner, M. A. *J. Am. Chem. Soc.* **2013**, *135*, 3953.
(34) Thazhathveetil, A. K.; Trifonov, A.; Wasielewski, M. R.; Lewis, F. D. *J. Am. Chem. Soc.* **2011**, *133*, 11485.
(35) Genereux, J. C.; Barton, J. K. *Chem. Rev.* **2010**, *110*, 1642.
(36) Lewis, F. D.; Wu, Y.; Zhang, L.; Zuo, X.; Hayes, R. T.; Wasielewski, M. R. *J. Am. Chem. Soc.* **2004**, *126*, 8206.
(37) Melhuish, W. H. *J. Phys. Chem.* **1961**, *65*, 229.
(38) Henry, E. R.; Hofrichter, J. *Methods Enzymol.* **1992**, *210*, 129.
(39) Zamis, T. M.; Parkhurst, L. J.; Gallup, G. A. *Comput. Chem.* **1989**, *13*, 165.